Bulgarian Academy of Sciences. Space Research Institute.
Aerospace Research in Bulgaria. 23, 2009, Sofia

ATMOSPHERIC GRAVITY WAVES ASSOCIATED WITH THE SOLAR TERMINATOR'S MOVING THROUGH THE EARTH'S UPPER ATMOSPHERE

Georgii Lizunov[1], Alla Fedorenko[1], Ludmil Bankov[2], Any Vassileva[2]

[1] Space Research Institute - NSAU, Ukraine
e-mail: liz@ikd.kiev.ua
[2] Space Research Institute –Bulgarian Academy of Sciences
e-mail: ludmil.bankov@gmail.com

Abstract

Upper atmosphere dynamical response to moving solar terminator is investigated based on direct satellite measurements. The observations on Atmosphere Explorer-E are analyzed over the period when the satellite was positioned on circular near-equatorial orbit with inclination of $i = 19.7°$ and height of 250-300 km. It is shown that the terminator generates large-scale atmosphere gravity waves (AGW) and travelling ionosphere disturbances (TID) with the following parameters: 1) the horizontal wavelength is close to 1200-1600 km; 2) the calculated period is about 50 minutes; 3) the duration of AGW/TID train is four-six wave periods; 4) the relative amplitude of the AGW is several percents; 5) the relative amplitude of TID at sunrise terminator is about several percents, at sunset terminator – up to ten percents; 6) plasma density oscillations $[O^+]$ are generated in opposite phase with the oscillations of the main neutral components $[N_2]$, $[O]$; molecular ion densities $[NO^+]$ and $[O_2^+]$ oscillate in phase with the neutrals. The obtained experimental results are interpreted based on the theory of AGW propagation in multi-component gas medium. It is shown that the amplitude and phase distinctions of the oscillations of the atmospheric components (including the main ionic component O^+) are caused by differences in the vertical distributions of atmosphere gases above the turbo-pause.

Introduction

The first theoretical suggestion on the possible generation of Atmospheric Gravity Waves (AGWs) by the solar terminator is made in [1]. The ionospheric response to the moving terminator as a Travelling

Ionospheric Disturbance (TID) has been the subject of a great number of ground-based observations [2, 3 and references therein]. In the present work, we study the process of wave generation at the solar terminator based on *in situ* measurements carried out on the *Atmosphere Explorer-E* (AE-E) satellite at the low latitude bottom side of F-region ionosphere. A diagram of the relative geometry of the AE-E orbit and the solar terminator position is shown in Fig.1.

In the Sun-Earth reference frame, neutral atmosphere co-rotating with the Earth crosses a steady terminator, which leads to the generation of a wave in associated day/night transition zone. As can be seen from Fig.1, in a given season, subsequent AE-E orbits cross the terminator zone and the wavelike structures attached to it in quite a similar manner. This in fact allows us to observe this wave with the periodicity of the satellite motion. In the late 70's and early 80's, complex satellite experiments were carried out to study ionosphere-thermosphere-magnetosphere interactions, such as *Atmosphere Explorer-C, D, E*, *Dynamics Explorer-B* etc. [4]. In the present work, we use AE-E data within the period of circular orbit at an altitude of 250-350 km and orbital inclination of 19.7^{o}. Such an orbital configuration of AE-E corresponds quite well to the studied terminator processes. First, satellite AE-E is at low Earth orbit (LEO) and second, because of the low orbital inclination, it crosses the wavelike train generated by the terminator (Fig.1). Most of the later "ionospheric" satellites, including nowadays DEMETER satellite, are launched at higher orbits (more than 700 km), well above the heights of AGW/TID propagation.

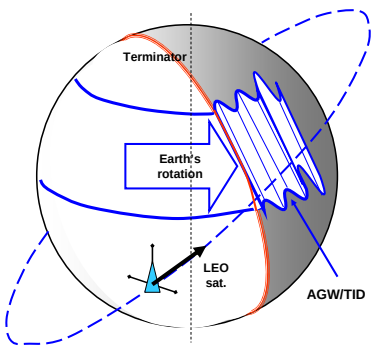

Fig.1. A diagram of Low Earth's Satellite observational opportunities at the terminator is shown. The relative position of the satellite's orbit, the terminator and the generated wavelike structures changes with time only due to the orbital precession.

Optically, solar terminator is a surface, which divides daylight from night-time part of the atmosphere. At altitude of 300 km, the angle between the horizon and the optical terminator's surface is about 10°, the thickness of the twilight zone is 55 km and the equatorial velocity of the terminator relatively to the Earth's surface is $V_{ST} = 450$ m/s. We will call AGW/TID generation zone the physical terminator, which is spread eastward of the optical terminator with characteristic width $L \sim 1500$ km (nearly one-hour band in local time). The relative configuration of the optical and physical terminators is shown in Fig.2.

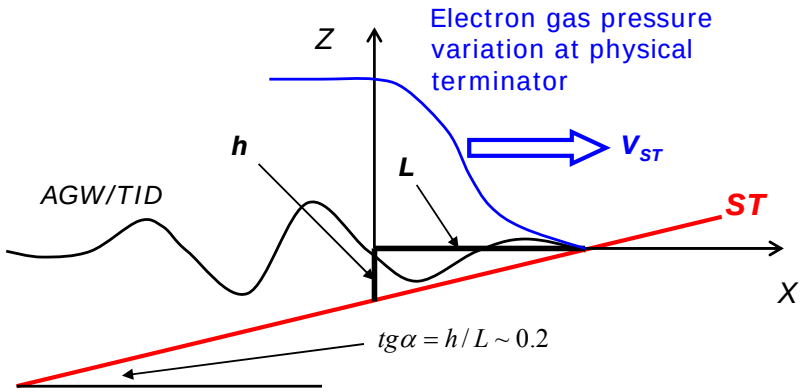

Fig. 2. Structure of the sunrise terminator. ST – optical terminator, between sunlight and dark night-side atmosphere. Wave generation appears in the region of solar energy accumulation with horizontal length scale L (at physical terminator).

The physical mechanisms of solar energy absorption which lead to the generation of atmospheric fluctuations are discussed in [5, 6]. At large solar zenith angles (at the terminator more than 90°), the main part of the energy in the UV band dissipates higher than 200 km. Because of the AGW's small group velocity, wave propagation upward and downward from the region of maximum absorption cannot explain the existence of neutral atmospheric disturbances at adjacent altitude layers, which are obviously generated independently by the terminator.

The structure of the work is as follows: Chapter 1 provides a simple explanation of the data processing procedure applied to the AE-E data; Chapter 3 contains a case study of several selected events; and Chapter 4 gives a theoretical interpretation of the observations.

1. Data processing technique

Here we use AE-E data taken from the database of the *National Space Science Data Center*, web-site: <http://nssdc.gsfc.nasa.gov/atmoweb>. As relevant parameters of the atmosphere around the F2 layer height have been chosen:

- neutral O and N_2 density;
- neutral temperature T_n;
- O^+ ion density;
- NO^+ и O_2^+ molecular ion density.

To study the wavelike disturbances generated by the moving terminator, we use a special data processing algorithm. While phase velocity of the AGW (hundreds of m/s) is small compared to the satellite orbital velocity of $V_{sat} \approx 8$ km/s, the frequency of the observed atmospheric disturbances is given by the wavelength spectrum: $\omega' = \omega - k_x V_{sat} \approx -k_x V_{sat}$, where ω – frequency of the AGW/TID in the stationary reference frame, $k_x = 2\pi / \lambda_x$ – wave vector component along the satellite's track, λ_x – horizontal wavelength. The smallest observable wavelength $\lambda_{\min}$ is determined by the Naiquist scale $\lambda_{\min} = 2 \cdot V_{sat} t_{sampl}$, where t_{sampl} is the data sampling time interval. In the case of AE-E, $t_{sampl} = 15$ s, $\lambda_{\min} = 240$ km. The maximal wavelength depends on the data processing method. We reduce our analysis to $\lambda_{\max} \sim 2000$ km in order to locate large scale AGW/ TID [7, 8].

The major problem of the undertaken data processing is related with wave selection against abrupt changes of the atmospheric parameters. Let us examine an example, which appears in sunrise ionosphere. Close after the terminator, within few hours, in the F-region, plasma density grows by more than an order of magnitude. In the same time, the terminator generates plasma fluctuations, a TID with relative amplitude of several percents, which forms a "small ripple" on the base gradient plasma density. In this case, to recognize the AGW, it is correct to extract trends from the data before calculating the spectral characteristics.

2. Data analysis

Data analysis of AE-E shows that in the morning hours after sunrise (for example 6-11 a.m. local time) and in the evening, after sunset (7-12 p.m. local time), a relative increase in wave activity is observed, which is

manifested as variations in the density and temperature of the different atmospheric species.

In Fig.3, a typical example of the wavelike disturbance on sunrise terminator is shown. Upon elimination of the large scale trends, we select the variations of the neutrals (AGW) and plasma (TID) with relative amplitudes $\delta[O]/[O] \sim 5\%$, $\delta[O^+]/[O^+] \sim 10\%$. It has to be pointed out that the main neutral components [O] и [N_2] vary in synchrony but with different relative amplitudes (amplitude ratio ~ 2). The wavelet transformation shows the presence of horizontal wavelength (about $\lambda_x = 1250$ km) and localizes the time interval within the observed wavelike activity (6-10 a.m. LT).

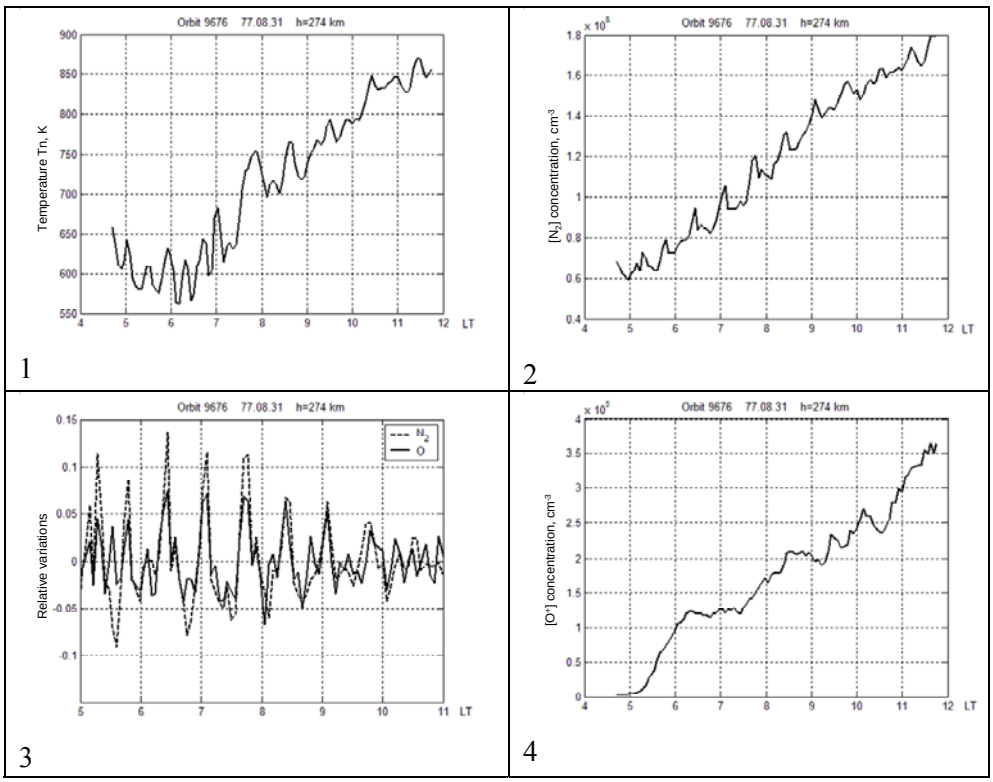

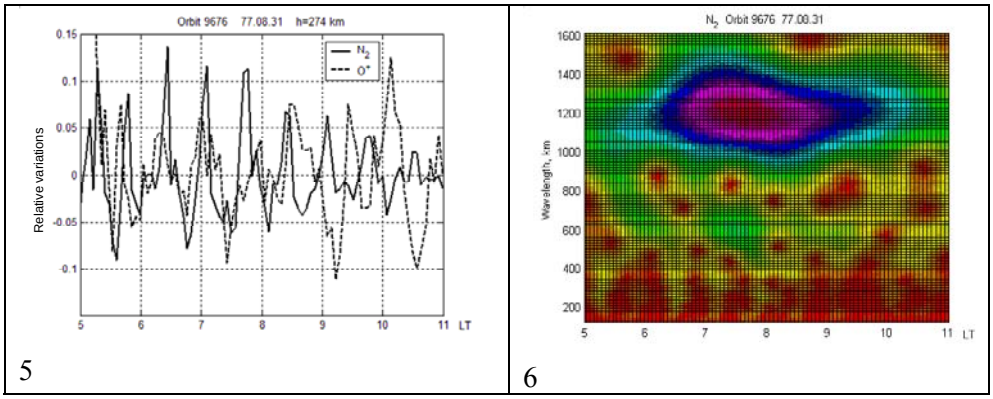

Fig.3. Atmospheric parameters behaviour at sunrise terminator, as observed at orbit 9796. Panels 1,2,4 – represent neutral temperature T_n, neutral density of $[N_2]$ and ion density of $[O^+]$; Panel 3 – smoothed relative variations of the neutral components; Panel 5 – neutral and plasma components; Panel 6 – wavelet spectrum of $[N_2]$ density variations

An example of the evening terminator fluctuations is shown in Fig.4. Upon elimination of the trends, relative variations in the neutrals and plasma are selected with characteristic size $\lambda_x \approx 1400$ km. The density of the major ion $[O^+]$ varies in anaphase with molecular ion density $[O^+_2]$ and $[NO^+]$. Latest in amplitude and phase follow the main neutral components.

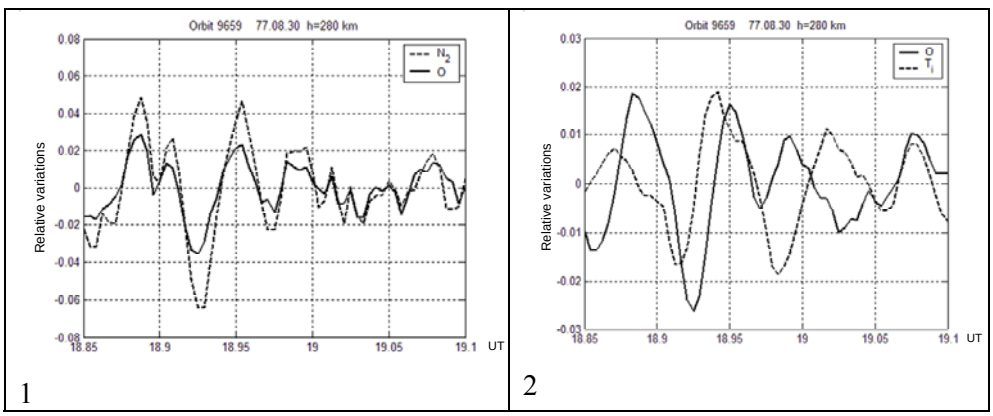

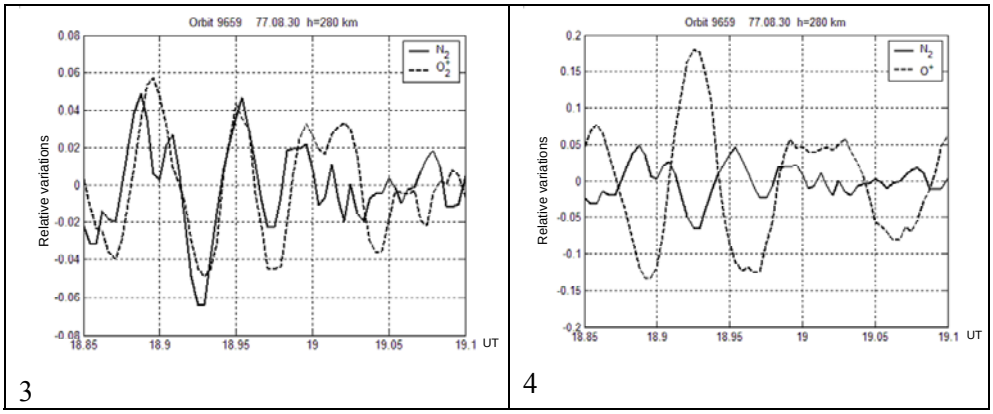

Fig.4. AGW/TID at evening terminator (7-9 p.m. LT). Panel 1,2 – relative density variations of the main neutral components and ion temperature Ti; Panel 3,4 – relative variations of different ion species vs. main neutral component [N_2] fluctuations

Following this procedure, we examined 8 cases at the terminator, which are summarized on Table 1. For sunrise and sunset conditions, the wavelengths almost coincide, the length of the wavelike zones of AGW/TID and the relative amplitudes of the AGW. The main peculiarity of the evening events is their larger plasma response amplitudes.

Table 1

Data	Orbit	h, km	Local time	Relative fluctuations, %						V_z, m/s	λ_x, km
				[N_2]	[O]	T_n	[O^+]	[NO^+]	[O_2^+]		
Dusk terminator											
77.04.23	7581	255	20-1^h	4	2	2	20	-	-	5	1400 + 2800
77.04.23	7583	255	20-3^h	6	3	3	15	-	-	7	1440
77.08.30	9659	280	19-24^h	5	3	-	20	5	5	10	1600
Dawn terminator											
77.04.19	7514	257	4-11^h	3	1,5	1	1	-	-	5	1600
77.07.28	9135	266	4-11^h	-	-	3	10	-	-	-	1500
77.08.31	9676	274	5-11^h	10	5	5	10	-	-	-	1250
77.10.08	10290	281	4.5-9.5^h	3	2	2	3	-	-	-	1400
78.03.19	12874	317	6-11^h	2	1	1	3	2	2	-	1300

To illustrate the repeatability of the behaviour of wavelike structures at the selected terminator described above, an additional example is shown in Fig. 5. One can see wave trains associated with evening terminator

observed from three different passes of AE-E at altitude of ~320 km in the longitudinal zone with geographic longitudes from -65° to -25°, during three subsequent days from March 10 to March 12, 1978. Data are matched along the local terminator position ST. Total ion density variations taken from IDM/RPA instrument have quite similar shape in the post sunset parts of the orbits on panel (a) on the left side of Fig.5. The dotted lines mark the smoothed density profile to extract the trends from data. In Fig.5 (b), the spectral power density of the smoothed profiles is shown for these three cases. Relative wavelength is about $\lambda_x = 1250$ -1400 km.

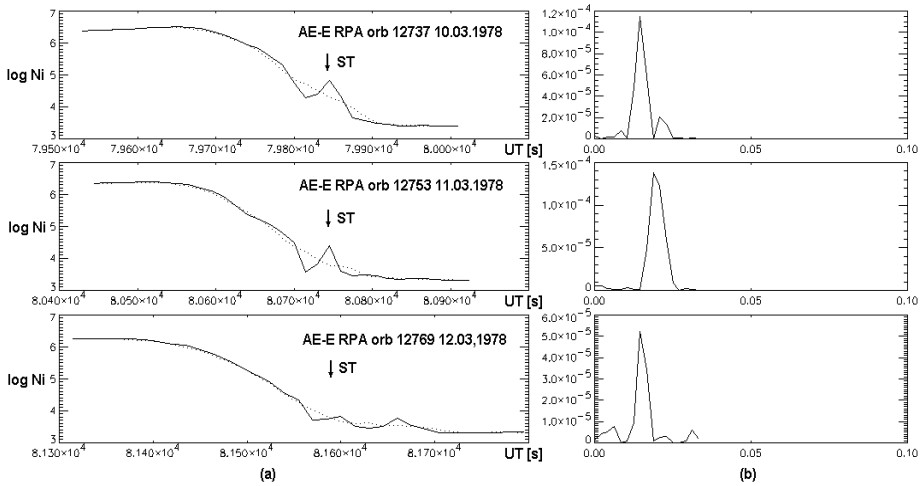

Fig.5. RPA Ni density profiles as taken from three equatorial passes through the terminator zone of AE-E during three subsequent days at height of ~320 km

3. Discussion

The theory of AGW in multi-component medium is the subject of [9, 10], where it is shown that the amplitude and phase of fluctuations for different sorts of gases are different. This effect has been observed experimentally on Atmosphere Explorer-C data and discussed in [11, 12]. Let us examine in details the generation mechanism of fluctuations in the air density of propagating AGW. AGW compression phase appears because of upwelling of the dense bottom layer of the atmosphere. In the same way, rarefied phase of AGW appears when low density air from upper levels moves downward in the atmosphere.

Let us consider that the motion of elementary air volume is slow enough, so the air pressure in the volume equalizes with the surrounding atmosphere. In this case, density changes could be written as follows:

$$(1) \qquad \delta\rho_s(t) = c_s^{-2}\delta p_s(t) = c_s^{-2}\delta\left(p_0 e^{-z(t)/H}\right) \approx -\frac{\delta z(t)}{\gamma \cdot H}\rho(z),$$

where c_s – sound velocity, $p(z) = p_0 e^{-z/H}$, $\rho(z) = \rho_0 e^{-z/H}$ – barometric distribution of atmospheric pressure and γ – adiabatic factor, $\delta z = \delta z(t)$ – vertical displacement of the air volume. Density variation at a given height is equal to the difference of upwelling volume $\rho_s(z) = \rho(z - \delta z) + \delta\rho_s$, and undisturbed air density $\rho(z)$:

$$(2) \qquad \delta\rho(t) = \rho_s(z) - \rho(z) = \delta\rho_s - \delta\left(\rho_0 e^{-z/H}\right) \approx \frac{\gamma - 1}{\gamma}\frac{\delta z(t)}{H}\rho,$$

which leads to

$$(3) \qquad \frac{\delta\rho(t)}{\rho} = \frac{\gamma - 1}{\gamma}\frac{\delta z(t)}{H}.$$

The latest expressions relate the relative AGW amplitude $A = \delta\rho/\rho$ with the amplitude of vertical displacement of the particles δz.

Repeating the procedure for the "α" sort of gases and taking in account that, after rarefaction or compression of the mixed gases, the density of the individual components changes in a proportional way $\delta\rho_{s\alpha}/\rho_{s\alpha} = \delta\rho_s/\rho_s$ and that, above turbo pause, different components follow individual vertical distribution corresponding to scale H_α, one can write:

$$(4) \qquad \frac{\delta\rho_\alpha}{\rho_\alpha} = \left(\frac{H}{H_\alpha} - \gamma^{-1}\right)\frac{\delta z}{H} = \frac{\gamma H/H_\alpha - 1}{\gamma - 1}\frac{\delta\rho}{\rho}.$$

Expressions (3), (4) are obtained under the following simplifying assumptions: (i) AGW propagation does not disturb hydrostatic distribution of atmospheric pressure $p(z) = p_0 e^{-z/H}$, $p(x, y) = const$, (ii) different atmospheric gases move in AGW in the same way. More strict estimations made in [9, 13] lead to negligible quantitative corrections in relations (7), (8) which could be neglected in our further treatment.

In AE-E observations at 250…300 km, the predominant atmospheric component is atomic oxygen (almost 90% of total density), where scale height of the multi component atmosphere $H \approx H_O \approx 50$ km, adiabatic

factor $\gamma = 5/3$ (single component gas). For the characteristic AGW amplitude of $A = \delta[O]/[O] \sim 0.02$, the amplitude of the vertical displacement of layers following (3) becomes $\delta z \sim 2$ km. The next atmospheric components, molecular nitrogen and helium, have density ratio $[O]:[N_2]:[He] = 100:10:1$ and scale height ratio $H_O : H_{N2} : H_{He} = 1:1.75:0.25$. From equation (4), the amplitudes of individual gas disturbances become

$$\frac{\delta[N_2]}{[N_2]} \approx 3\frac{\delta[O]}{[O]}, \quad \frac{\delta[He]}{[He]} \approx -\frac{\delta[O]}{[O]}, \tag{5}$$

which is in good agreement with AE-E observations. Note that helium density variations are opposite to the variations of background component.

On some orbits, AE-E provided measurements of neutral wind vertical component of the velocity V_z (see. Table 1). This allows us to calculate the period of observed AGW from experimental data. While $V_z = \delta\dot{z} = i\omega\delta z$, relation (3) represents frequency, relative AGW amplitude and vertical wind velocity:

$$\omega = \frac{\gamma - 1}{\gamma}\frac{V_{zm}}{H}A^{-1}, \tag{6}$$

where V_{zm} – is amplitude of velocity fluctuations. The calculated periods of AGW are about 50…55 min, which is well supported by theoretical estimations.

These estimations, concerning the various effects on neutral atmosphere from propagating AGW, also give us a key to understand plasma response to AGW. It has to be pointed out here that ion density disturbances in relative units usually prevail over neutral atmosphere response to AGW. This is demonstrated pretty well by the enhanced AGW amplitude in plasma density in the night time hemisphere where the amplitudes of TID reach up to ten percent.

As it is well known, at night time conditions, F-region plasma support originates from downward diffusion of O^+ ions from topside ionosphere [14]. Recombination processes of molecular nitrogen at altitudes of about 200…300 km lead to the formation of steep gradient in the vertical ion density profile $n_p(z)$. The dynamics of the F-region predominant O^+ ions is described by the continuity equation:

(7) $$\frac{\partial[O^+]}{\partial t}+\frac{\partial}{\partial z}\left(V_D\cdot[O^+]\right)=-a[N_2][O^+],$$

where V_D is vertical plasma drift velocity, a – ion-neutral recombination coefficient, term $\tau=(a[N_2])^{-1}$ – lifetime of O^+ ions. Assuming $\partial/\partial t=0$, one can evaluate the quasi-stationary vertical distribution of night time O^+ ion density:

(8) $$[O^+]=n_p(z)=n_{p0}\exp\{\frac{H_{N2}}{H_p}\left(1-e^{(z_0-z)/H_{N2}}\right)\},$$

where $H_p=(a[N_2])^{-1}|_{z=z0}\cdot V_D$ – drift length of O^+ ions for lifetime τ. Near F maximum vertical profile could be approximated by exponential function (9):

(9) $$n_p(z)\approx n_{p0}\exp\{\frac{z-z_0}{H_p}\},\ \text{while}\ |z-z_0|<H_{N2}.$$

Thus, drift length H_p plays the role of plasma distribution vertical scale (ionospheric scale height). If $z_0=300$ km, $V_D=10$ m/s, $\tau=(aN_2)^{-1}|_{z=z0}=10^3$ s, scale height becomes $H_p=10$ km.

The influence of AGW on plasma dynamics in the F-region is described by equation (7) where the following replacements can be made: $aN_2\to aN_2+\delta(aN_2)$ (changing recombination background under the influence of AGW) and $V_D\to V_D+\delta V_i$ (neutral particles effectively drug ions). Estimations show that, beneath h_mF2 altitude, especially in the steep ion density gradient zone [11], the latest term prevails. Because of the high ion-neutral collision frequency at these heights, ions move along the magnetic field lines with the speed of neutrals, and in parallel, ions drift perpendicularly, driven by perpendicular electric field [14, 15]. Thus, $\delta V_i\sim\delta V_n$, which coincides with *in situ* velocity measurements on AE-E. In this case, the estimation of plasma density variations leads to expression (4) with negative plasma scale height $H_\alpha=-H_p$ (while $z<h_mF2$ plasma density increases with altitude):

(10) $$\frac{\delta[O^+]}{[O^+]}\sim-\frac{\gamma H/H_p+1}{\gamma-1}\frac{\delta[O]}{[O]}.$$

In accordance with (10), ion density fluctuations occur in anti-phase with AGW with larger relative amplitudes. If we assume $H = 50$ km, $H_p = 10$ km, relative O^+ variations become

$$\left|\frac{\delta[O^+]}{[O^+]}\right| = 15 \cdot \left|\frac{\delta[O]}{[O]}\right|. \quad (11)$$

In contrast to the major O^+ ions, molecular NO^+ and O_2^+ ion motion caused by neutrals in the space/time scale of AGW is negligible. AGW propagation affects molecular ions only by reducing background recombination levels, because their photochemical lifetime at these altitudes is less than one minute. Relative variations of molecular ions do follow neutral density fluctuations (see Fig. 5.3) where:

$$\frac{\delta[NO^+]}{[NO^+]} \sim \frac{\delta[N_2]}{[N_2]}, \quad \frac{\delta[O_2^+]}{[O_2^+]} \sim \frac{\delta[O_2]}{[O_2]}. \quad (12)$$

Conclusions

In the present paper, wavelike processes at the terminator are studied for the first time by means of *in situ* satellite observations. Atmosphere Explorer-E satellite provided both neutral and charged particle measurements in the Earth's atmosphere, which permits *in situ* study of AGW and TID, their interactions with background atmospheric species. For the period of the data used here, AE-E measurements cover equatorial ionosphere at altitude 250…300 km, beneath F-region maximum.

As shown by experimental data, in the morning hours after sunrise (6…11^h local time) and evening hours after sunset (19…24^h), intensification of the wavelike activity in the various atmosphere components is observed, evidencing of large scale generation of AGW/TID by moving terminator. The main persistent characteristics of these fluctuations could be summarized as follows:

- Horizontal wavelength 1400…1600 km;
- Estimated period 50…55 min;
- AGW/TID train of 4…6 wave periods;
- Relative AGW amplitudes of few percents;
- Relative morning TID amplitudes of few percents, and evening TID amplitudes greater than ten percents;
- Relative ion density variations prevail over the corresponding neutral density fluctuations. At night $[O^+]$ density behaviour is in

anti-correlation with the variations in the main neutral components such as $[N_2]$, [O].

– Variations in $[NO^+]$ and $[O_2^+]$ molecular ions do follow neutral atmosphere fluctuations.

The amplitude and phase relationships between the different atmospheric components presented in this paper do correspond to the main behaviour of AGW above turbopause. Note that the changes in volume density in the presence of AGW correspond to the upward motion of dense air layers and downward motion of rarefied layers from the top. The dimensionless parameter referred to density variation of gas component $\delta\rho_\alpha$ corresponds to the ratio of vertical displacement of layer to the scale height of the given component $\delta z / H_\alpha$. The heavier is the gas component (i.e. as small is H_α), the higher is the relative density variation. Below ionospheric maximum $z < h_m F2$ plasma density increases with height which leads to negative scale heights at these altitudes. As a result, plasma and neutral density have opposite variations and plasma variations are larger than relative amplitudes in AGW.

Ionospheric plasma response to AGW propagation discussed here is of great importance, because ground-based and space-borne AGW measurements concern mostly the registration of plasma effects of AGW instead of neutral ones.

References

1. Beer T. Supersonic generation of atmospheric waves //Nature. – 1973. – V.242, N5392. – P.34.
2. Galushko V. G., V. V. Paznukhov, Y. M. Yampolski and J. C. Foster. Incoherent Scatter Radar Observations of the AGW/TID Events Generated by the Moving Solar Terminator // Ann. Geophys. –1998. – Vol.16. – p. 821-827.
3. Бурмака В. П., В. И. Таран, Л. Ф. Черногор. Результаты исследования волновых возмущений в ионосфере методом некогерентного рассеяния //Успехи современной радиоэлектроники. – 2005. – №3. – С.4-35.
4. Dalgarno A., W. B. Hanson, N. W. Spencer and E. R. Schmerling. The Atmosphere Explorer mission // Radio. Sci. – 1973. –V. 8. –P. 263-273.
5. Сомсиков В. М. Солнечный терминатор и динамика атмосферы. – Алма-Ата: Наука, 1983. – 192 с.
6. Сомсиков В. М. Волны в атмосфере, вызванные движением солнечного терминатора (обзор) //Геомагнетизм и аэрономия.– 1991. – Т.31, № 1, с.1-12.

7. G e o r g e s T. M. HF Doppler studies of travelling ionospheric disturbances // Journal of Atmospheric and Terrestrial Physics. – V. 30. – P. 735-746.
8. F r a n c i s S. H. Global propagation of atmospheric gravity waves: a review// Journal of Atmospheric and Terrestrial Physics. –1975. – V. 37. – P. 1011-1054.
9. D e l G e n i o A. D., G. S c h u b e r t, J. M. S t r a u s. Gravity wave propagation in a diffusively separated atmosphere with height-dependent collision frequencies// J. Geophys. Res. –1979 – V.84,NA8 – P.4371-4378.
10. I n n i s J. L and M. C o n d e. Characterization of acoustic-gravity waves in the upper thermosphere using Dynamics Explorer 2 Wind and Temperature Spectrometer (WATS) and Neutral Atmosphere Composition Spectrometer (NACS) date // J. Geophys. Res. –2002. – Vol.107, № A12. – SIA 1-21.
11. R e b e r C. A., A. E. H e d i n, D. T. P e l z, W. E. P o t t e r and L. H. B r a c e. Phase and amplitude relationships of wave structure observed in the lower thermosphere // J. Geophys. Res. –1975. –V.80. –P. 4576-1975.
12. P o t t e r W. E., D. C. K a y s e r and K. M a u e r s b e r g e r. Direct measurements of neutral wave characteristics in the thermosphere //J. Geophys. Res. – 1976. – V.81. – P.5002.
13. M a k h l o u f U., E. D e w a n, J. R. I s l e r and T. F. T u a n. On the importance of the purely gravitationally induced density, pressure and temperature variations in gravity waves: Their application to airglow observations //J. Geophys. Res. – 1990. – V.95. – P. 4103-4111.
14. Б р ю н е л л и Б. Е., А. А. Н а м г а л а д з е. Физика ионосферы. – М.: Наука, 1988. – 527 с.
15. K e l l e y M. C. The Earth's Ionosphere Plasma Physics and Electrodynamics // Academic Press. Inc. International Geophysics Series –1989. –V.43. – 487 p.

ГРАВИТАЦИОННИ ВЪЛНИ В АТМОСФЕРАТА, СВЪРЗАНИ С ДВИЖЕНИЕТО НА СЛЪНЧЕВИЯ ТЕРМИНАТОР ПРЕЗ ВИСОКАТА АТМОСФЕРА НА ЗЕМЯТА

Г. Лизунов, А. Федоренко, Л. Банков, А. Василева

Резюме

Чрез използването на данни от непосредствени (in situ) измервания на спътника Atmosphere Explorer - E са изследвани ефектите от движението на слънчевия терминатор във високата атмосфера. Анализирани са данните от приборите RPA (Retarding Potential Analyzer) и NACE (Neutral Atmospheric Composition Experiment) за периода на кръгова екваториална орбита на спътника с инклинация $i = 19.7°$ и

височина 250-300 km. Показано е, че при движението си през неутралната атмосфера, слънчевият терминатор генерира крупномащабни атмосферни гравитационни вълни (АГВ) и движещи се йоносферни смущения (ДИС) със следните параметри: 1) хоризонтална дължина на вълната около 1200-1600 km; 2) период около 50 минути; 3) характерен хоризонтален размер на вълновия пакет АГВ/ДИС от четири до шест вълни; 4) относителната амплитуда на АГВ е от порядъка на няколко проценти от концентрацията; 5) относителната амплитуда на ДИС около изгревния терминатор е от порядъка на няколко процента, докато за вечерния терминатор надминава десет процента; 6) вариациите в концентрацията на $[O^+]$ са в противофаза с вариациите в преобладаващите неутрални компоненти $[N_2]$, [O]; 7) молекулярните йони $[NO^+]$ и $[O_2^+]$ осцилират във фаза с неутралите. Получените експериментални резултати са интерпретирани в светлината на теорията на разпространение на АГВ в мултикомпонентна среда. Показано е, че особеностите в разпределението на амплитудите и фазите за осцилациите на неутралните и заредените компоненти в атмосферата се дължат на разликите във вертикалното им разпределение над турбопаузата.